การผลิตชิ้นส่วนรถยนต์สมรรถนะสูงด้วยกระบวนการฉีดหล่อโลหะผง

นางสาวอดิกานต์ ทองสอาด

PRODUCTION OF HIGH PERFORMANCE AUTOMOBILE PARTS BY THE METAL INJECTION MOLDING (MIM) PROCESS

Miss Adikarn Tongsa-ad

Thesis Title   Production of High Performance Automobile Parts by The Metal Injection Molding (MIM) Process
By   Miss Adikarn Tongsa-ad
Field of Study   Metallurgical Engineering
Thesis Advisor   Sawai Danchaivijit, Ph.D.
Thesis Co-advisor Ittipon Diewwanit, Sc.D.

_____
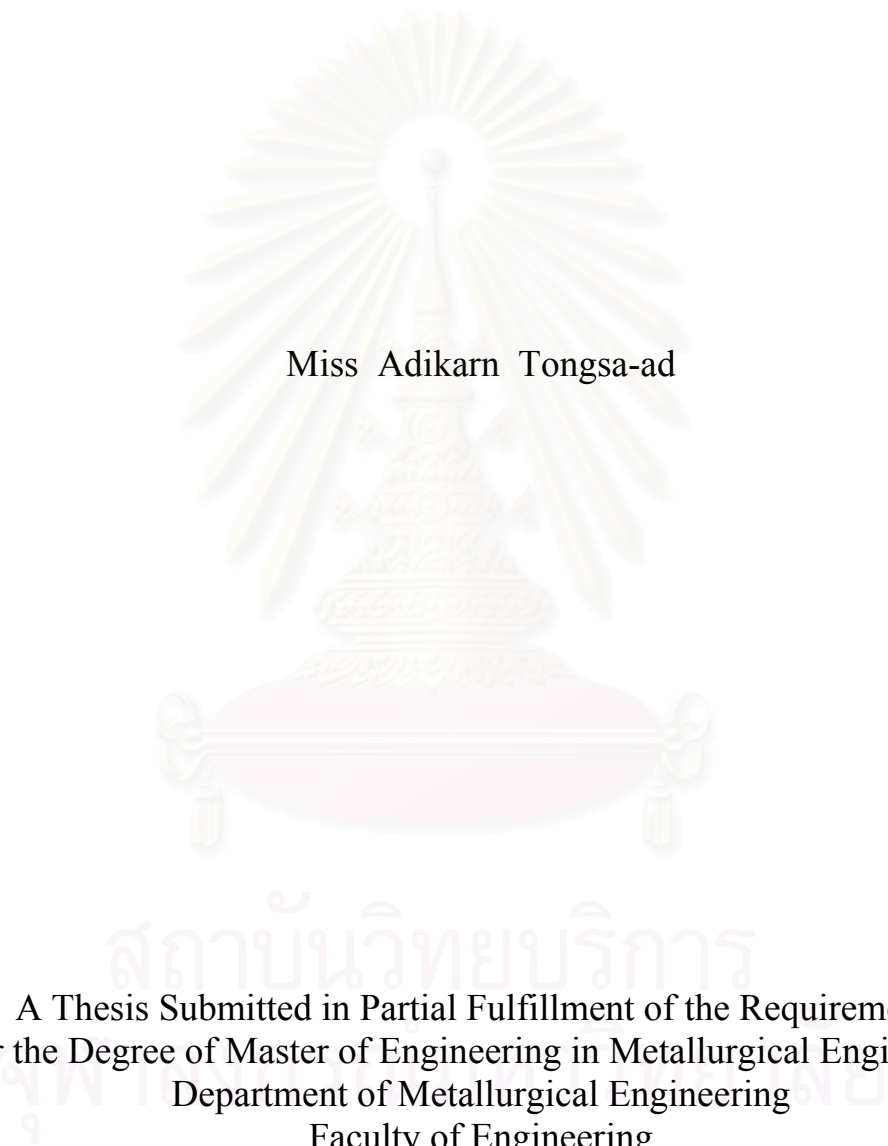
Accepted by the Faculty of Engineering, Chulalongkorn University in Partial Fulfillment of the Requirements for Master's Degree

…………………………….... Dean of Faculty of Engineering
(Professor Somsak Panyakeow, Dr.Eng.)

THESIS COMMITTEE

…………………………….... Chairman
(Associate Professor Prasonk Sricharoenchai, D.Eng.)

…………………………….... Thesis Advisor
(Sawai Danchaivijit, Ph.D.)

…………………………….... Thesis Co-advisor
(Ittipon Diewwanit, Sc.D.)

…………………………….... Member
(Assistant Professor Sumalee Vongchan, Ph.D.)

Effects of various processing parameters in the metal injection molding (MIM) process were investigated in order to study the fabrication of selected automobile part, splined coupling, through MIM process. 430L stainless steel powder and 40 vol% PAN-250 binder were mixed in a twin-screw kneader. The motor speed of 122 rpm was selected. The optimized molding conditions for tensile specimens and splined coupling were selected. The optimized debinding condition for tensile specimens was debinding temperature of 310-360°C in flowing air with fan for 30 hours which achieved 94-99%extraction.   The sintering conditions of 1195°C in $N_2+70\%H_2$ atmosphere and 1250°C, 1300°C, 1350°C in hydrogen atmosphere were used. At 1195°C, the sintering was not complete. At 1250°C, 1300°C and 1350°C, the sintering reached final stage and achieved the maximum density of 95.82% theoretical density. Physical and mechanical properties of the sintered tensile specimens were tested and the results were discussed. The splined coupling could be formed though MIM process. However, sintered splined couplings had some distortions resulting in dimensional control problem.

Department   Metallurgical Engineering   Student's signature…………………..……

Field of study   Metallurgical Engineering   Advisor's signature………..…………….

Academic year 2000   Co-advisor's signature……………………

อดิกานต์ ทองสอาด : การผลิตชิ้นส่วนรถยนต์สมรรถนะสูงด้วยกระบวนการฉีดหล่อโลหะผง อ. ที่ปรึกษา : อ.ดร. ไสว ด่านชัยวิจิตร อ. ที่ปรึกษาร่วม : อ.ดร. อิทธิพล เดี่ยววณิชย์ ; 50 หน้า. ISBN 974-347-293-2

วิทยานิพนธ์ฉบับนี้เป็นการศึกษาปัญหา และผลกระทบของตัวแปรต่างๆ ในกระบวนการฉีดหล่อโลหะผง และ ทำการขึ้นรูปชิ้นส่วนรถยนต์คือ ข้อต่อแบบเฟืองภายใน (Splined Coupling) ด้วยกระบวนการฉีดหล่อโลหะผง ผงเหล็กกล้าไร้สนิมเกรด 430L และตัวประสาน PAN-250 ผสมกันในเครื่องนวดพลาสติก ความเร็วมอเตอร์ในการผสมคือ 122 รอบต่อนาที ของผสมที่ได้ถูกนำไปฉีดขึ้นรูปด้วยเครื่องฉีดพลาสติก ในขั้นตอนการฉีดขึ้นรูปเลือกความดันและอุณหภูมิในการฉีดที่เหมาะสมของชิ้นงานทดสอบแรงดึงและข้อต่อแบบเฟืองภายใน สภาวะการเผาไล่ตัวประสานที่ดีที่สุดคือ 310-360°C ในบรรยากาศที่มีพัดลมเป่าเพื่อการหมุนเวียนของอากาศภายในเตา ซึ่งได้อัตราการกำจัดตัวประสานที่ 94-99% ในขั้นตอนการเผาประสาน (Sintering) ใช้สภาวะการเผาที่ 1195°C ในบรรยากาศผสมระหว่างไนโตรเจนและไฮโดรเจน และ 1250°C, 1300°C และ 1350°C ในบรรยากาศไฮโดรเจน ที่อุณหภูมิ 1195°C การเผายังไม่สมบูรณ์ ส่วนที่อุณหภูมิ 1250°C, 1300°C, และ 1350°C การเผาเข้าสู่ขั้นสุดท้าย ได้ความหนาแน่นสูงสุด 95.82% ชิ้นงานทดสอบแรงดึงนำไปทดสอบคุณสมบัติทางกายภาพและคุณสมบัติเชิงกล สำหรับข้อต่อแบบเฟืองภายในสามารถขึ้นรูปด้วยกระบวนการฉีดหล่อโลหะผงได้ แต่จากการทดลองยังมีการบิดเบี้ยวของรูปร่างชิ้นงาน ซึ่งเป็นปัญหาต่อการควบคุมขนาดรูปร่าง

ภาควิชา	วิศวกรรมโลหการ	ลายมือชื่อนิสิต...
สาขาวิชา	วิศวกรรมโลหการ	ลายมือชื่ออาจารย์ที่ปรึกษา.................................
ปีการศึกษา	2543	ลายมือชื่ออาจารย์ที่ปรึกษาร่วม...........................

Acknowledgement

Contents

Chapter

List of Tables

List of Figures

Chapter 1

Introduction

Nowadays, the industrial development is growing rapidly. There are many researches of new fabrication process. Innovations in these industries emphasize improvement of yield from raw materials resource and on the production of products of improved quality such as density, tolerance, mechanical properties and reliability.

Powder Injection Molding (PIM) is a new manufacturing technology which combines Powder Technology and Plastic Injection Molding that has undergone considerable maturation over the past five years. This technology started in the late 1920s and become credible in the late 1970s. Currently, the technology is used to fabricate metallic, ceramic, and cemented carbide components. Overall industry growth is strong and expanding rapidly.[1]

Metal Injection Molding (MIM) is a technology for manufacturing complex, high volume ferrous parts. Metal powders are mixed with thermoplastic binders to form a homogeneous mixture. The feedstock is then molded at relatively low temperatures and pressures in conventional plastic injection molding machines. The molds are similar to those used in plastic injection molding. The molded green parts are then thermally processed in two steps. First, the binder is removed by evaporation in an operation called debinding. Next, the part is sintered at a temperature near the alloy melting point which densifies the part isotropically. Consequently, the part has high final density. The complex shape of the original molded part is retained throughout this process and close tolerances can be achieved.[2] Final properties of PIM materials rival those of most other forming processes.

The two principal reasons for choosing to use a PIM product are indentified as product uniqueness and product cost effectiveness.[3] Many high temperature materials are available via PIM, with stainless steel, alumina, silica, iron and various steels. This process is capable of wide size variations, with parts in production having final thickness as small as 0.1 mm and as large as 1 m.[1] The complex shape of the original molded parts is retained throughout this process, and close tolerances can be achieved. MIM is replacing both machined parts requiring multiple machining operations and investment cast parts.[2] These machining operations can be costly and are wasteful in term of material and energy. The cost saving achievable by

PIM are maximised for components which require dimensional tolerance control.

However, because of high initial tool cost, it is necessary to seek out complex shapes with high performance requirements and high production volumes for PIM.

About half of all production are the components for internal products. These products include orthodontic brackets, firearm components, microelectronic packages, wristwatch cases, wear component, and biomedical implants. On the other hand, the industry that forms custom parts for external applications is equally large. The custom components are used for computer disk drives, locks, hand tools, automotive parts, radiation shields, and many similar industrial components.[1] This process is used widely in automobiles but engines and transmissions represent the most significant areas of application.[3] The stainless steel market is also experiencing an upsurge in growth mainly due to automotive applications such as mirror mounts, sensor rings for antilock braking systems, and door hinge bushings.

Even though MIM process has many advantages, there is a generally poor understanding of this complex process. Since there is no study and development of MIM process in Thailand, the study of MIM process will be made. Considering the rapid expansion of automobile parts industries in Thailand, attempt will be made to study the formation of selected automobile parts through MIM process. The final objective of this work is to lay a foundation for advance research to apply MIM for a production of high performance automobile parts in Thailand in the near future.

Objectives

The objectives of this study were:

1. To study the problems and effects of various processing parameters in metal injection molding (MIM) process.
2. To study the formation of automobile parts through MIM process.

Scope

In this study, the water atomised stainless steel 430L powder and PAN-250 binder will be mixed in twin-screwed kneader with the powder loading of 60 vol%. The compound is then molded by plastic injection molding machine to be tensile specimens. The compact will be debound and then sintered. The process and properties of tensile specimens will be study as follow:

1. Study mixer in mixing process.
2. Study surface defects of injected specimens by evaluate standard deviation of density at different positions of specimens and appearance.
3. Study debinding temperature and atmosphere in debinding process by evaluate %extraction and appearance.
4. Study sintering temperature in sintering process and microstructure of the specimens sintered from MEL, Japan and Thai Sintered Product CO.,LTD., Thailand by evaluate %shrinkage, density, hardness, tensile strength.

The selected automobile parts, splined coupling, will be also made through MIM process. The parts will be mixed and injected in the laboratory and then debound and sintered at ATOMIX COPERATION CO.,LTD., Japan. The density and appearance will be evaluated.

Expected Benefits

1. Understanding of the processing method for high performance automobile parts through MIM process.
2. Basis research works which can be extended to the actual application in the automobile parts industries through advance application.

Chapter 2

Literature Review

2.1 Processing details

The steps involved in forming a component by PIM include the following : 1) selecting and tailoring a powder for the process; 2) mixing the powder with a suitable binder; 3) producing homogeneous granular pellets of mixed powder and binder; 4) forming of the part by injection molding in a closed die; 5) processing the formed part to remove the binder (debinding); 6) densifying the compact by high-temperature sintering; and 7) post-sintering processing as appropriate, including heat treatment or further densification.

This technology is practiced with many variations on this basic process. The binder is often a thermoplastic polymeric material. The amount of binder ranges from 15 to 50 volume percent of the mixtures. Small particles are used to aid sintering densification. The injection molding step is similar to that applied to conventional polymeric material, involving concurrent heating and pressurization cycles. After molding, removal of the binder from the powder compact can be a slow step with minimum component distortion or cracking. In sintering, the void space remaining after removal of the binder is eliminated with concomitant shrinkage.

2.1.1 Mixing process

Mixing is the first step in the preparation of the feedstock for molding. The quality of the feedstock is crucial, since deficiencies cannot be corrected by subsequent processing adjustments. The goals in mixing are to coat particles with the binder, the break up agglomerates, and to attain uniform distributions of binder and particle size throughout the feedstock. Best mixing occurs with a high shear, but not to the point where the work of mixing damages the particles or overheats the binder. A properly mixed material will consist of a homogeneous powder dispersion in the binder, with no internal porosity or agglomerates. In homogeneous feedstock can lead to uneven packing density and distortion of the final product. [4]

Loh et al [5] studied the mixing factors by using Haake Torque mixer. The feedstock homogeneity was assessed by various indexes as density, binder burnt-out, torque level during mixing and rheological characteristics. Based on the density and wt% binder burnt-out indexes, powder loading rate and speed of rotor blade are the top two important factors affecting feedstock homogeneity. The optimal mixing condition for binder PAN-31 that give the most homogeneous feedstock are mixing temperature of 60°C, mixing time of 70 minutes, powder loading of 10g/min, speed of rotor blade of 10 rpm, and type of rotor blade of cam.

Because the feedstock is typically pseudoplastic, the viscosity of the mixture will vary with shear rate. Good mixing requires that all regions be equally sheared. To attain this goal, several high-shear mixer designs are used for PIM feedstock preparation. These include planetary, single screw extruder, plunger extruder, twin screw extruder, twin cam, and sigma or z-blade mixers. Unfortunately, this design proves to be the most expensive. AS s consequence, the double planetary mixer is often selected but this mixer has fewer problems with scale-up, fill volume and cleaning than other designs. The feedstock had difficulty forming a homogeneous mixture. Consequently, the mixer is equipped with additional intensifiers or the feedstock is extruded after mixing. [4]

2.1.2 Injection molding process

Molding consists of heating the feedstock to a sufficiently high temperature such that they are melted, then forcing this melt into a cavity where it cools and assumed the compact shape. The objective is to attain the desired shape free of voids or other defects and with a homogeneous distribution of powder. [4] Since the defect population in the compact and the presence of distortion in sintering is highly dependent on the molding step, a key goal in studying the molding process is to ensure compact fabrication without defect.

Ji et al [6] studied defects in molding process. The qualities of molded parts were checked visually for surface defects and by X-ray radiography for internal defects. The defects include voids, cracks, weld lines, sink marks and powder-binder separation occur during injection molding. Most of these defects are caused by inappropriate process parameters. These defects can

be rectified by proper control of process parameters such as pressure and temperature in molding.

2.1.3 Debinding process

The binder must be removed from the molded parts prior to its densification by sintering, at the same time without causing any defects in green parts.
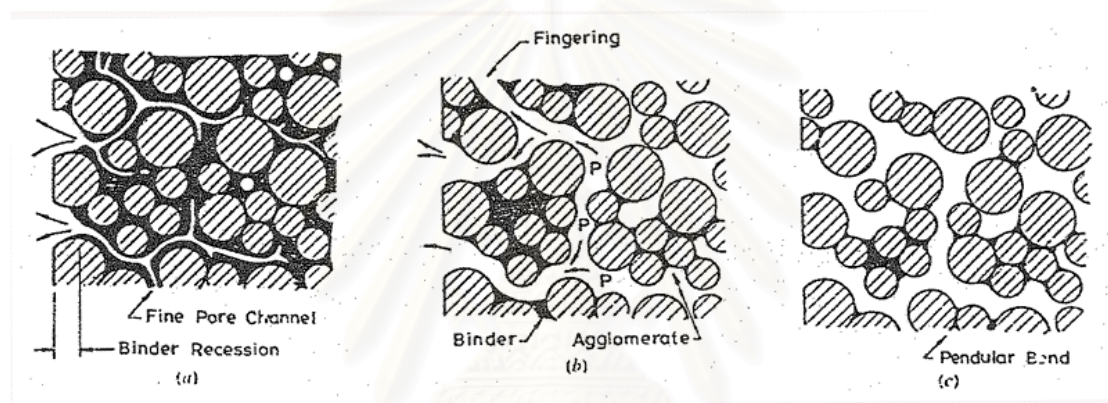
Figure 2.1 The schematics of binder distributions at the
(a) initial, (b) intermediate and (c) final stage of thermal debinding. [7]

Hwang et al [7] studied mechanisms of thermal debinding of powder injection molded parts from TGA curves of binder and SEM observations. There are 3 stages shown in figure 2.1.

In the initial stage of debinding, fine pores are developed uniformly within the molded article due to the decomposition of low-temperature binders. They provide paths for the decomposed gas to escape to the ambient. Hydraulic pressure develops because of the thermal expansion mismatch between the powder and binder. [8]

At the intermediate stage, binders become less viscous and are forced to the surface by internal gas pressure. Meanwhile, discrete islands of powder-binder agglomerate are formed due to capillary. Capillary forces move liquid binder from the center of the compact to the surface where

evaporation can continue. [8] Debinding is accelerated at this stage because there are more binder-vapor interfaces and larger pore channels.

The final stage involves thermal decomposition of remaining binder at higher temperature. [8] Remaining binder are trapped at contact points between powders forming pendular bond. Capillary forces are holding particle together starting at this stage and retain the shape of molded parts at the end of debinding.

Atmosphere control is vital to successful binder removal. Since the initial stages involve evaporation of the binder, there must be some mechanism to remove the evolved vapors from the area near the parts to prevent the binder from recondensing on the parts. Flowing gas is commonly used to transport vapors from the furnace at controlled flow rates. During the decomposition stage of debinding, the atmosphere in the furnace determines what reaction occurs and how much of the carbon residue is removed from the compact.

Moore et al [8] studied atmosphere control during debinding of powder injection molded parts. Inert atmosphere controlled the rate of binder removal over a wider temperature range compared with an oxidizing atmosphere. Argon produced the highest densities and lowest levels of residual contamination. Higher flow rates of Argon to reduce accumulations of volatilized binder control slumping.

Ji et al [9] studied effects of debinding parameters, debinding gas and flow rates, on metal injection molded parts. The best atmosphere was the mixture of 5% Hydrogen and 95% Argon which allows high binder removal and low residual carbon level. Meanwhile, the result shows that higher gas flow rate of 250 ml/min during debinding increase the binder removal and reduces residual carbon level.

However, oxidizing atmosphere is one choice for residual carbon control. Debinding in air is cheap and efficient but will oxidize a metallic part. [4]

2.1.4 Sintering process

Sintering is the bonding together of particles when heated to high temperature. There are 3 stages of sintering shown in figure 2.2.
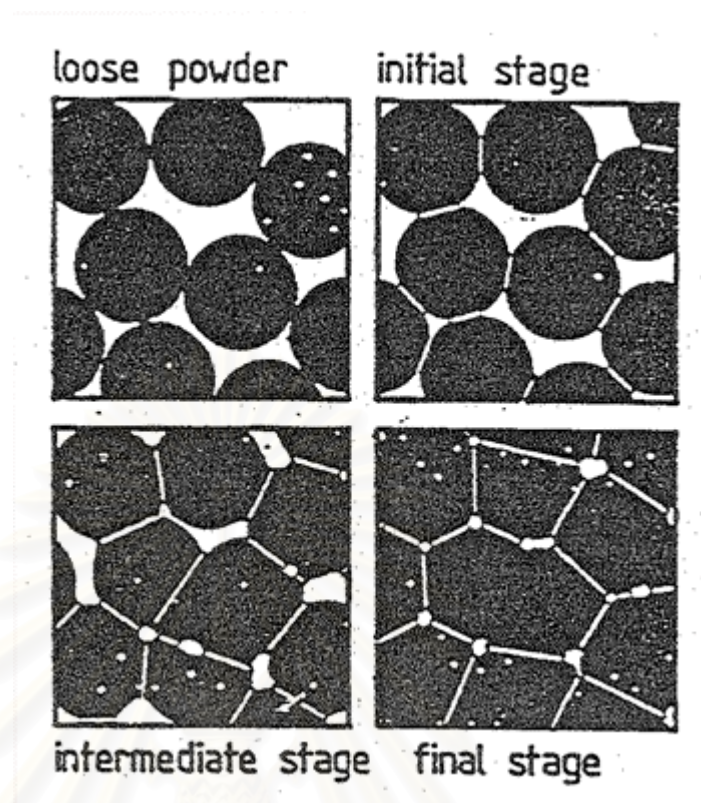
Figure 2.2 The development of the interparticle bond and
the changes in structure during sintering [4]

At the initial stage of sintering, the kinetics are dominated by the curvature gradients near the interparticle neck. The pore structure is opened and fully interconnected.

In the intermediate stage, the pore structure is much smoother and has an interconnected structure. Grain growth occurs in the latter portion of this stage. The density is between 70 and 92% of theoretical.

By the final stage of sintering, the pores are spherical and closed and grain growth is evident. Gas in the pores at this point will limit the amount of final stage densification. [4]

Loh et al [10] studied some sintering parameters of 316L stainless steel, i.e. temperature, heating rate and time, on the mechanical properties of the sintered parts.

At 1050°C, sintering has just started. At 1200°C, the sintering reached the intermediate stage. The sintering temperature is slowed down during final stage of sintering at 1350°C. The isolated pores start to form.

The results show that the density increases more significantly from 1050°C to 1200°C.

Slow heating rate encouraged more uniform grain formation and decrease in isolated parts. Slow heating rate of 5°C/min achieved maximum shrinkage.

Increase the sintering time results in enlarged grain growth that leads to lower hardness value. The low strength resulted from the reduction in grain boundaries.

From the results, slow heating rate of 5°C/min, sintering temperature more than 1200°C and sintering time of 60 minutes are the optimum sintering condition which encourage high amount of shrinkage and density.

Ji et al [11] studied some sintering factors of 316L stainless steel, i.e. sintering temperature and sintering atmosphere on final sintered density. Sintering atmosphere is the factor which affects the final density much more than other sintering factors. The size and number of pore of the parts which sintered in vacuum are smaller than the ones sintered in Nitrogen and in Argon. Optimum fractional final density of 96.14% of wrought material was achieved with sintering temperature of 1250°C and sintering in vacuum. Sintering in Argon and Nitrogen achieved fractional density of 94.62% and 94.80% respectively.

Sintering in Hydrogen at the temperature of 1260°C can achieved the sintered density of 97% of theoretical density. [13]

2.2 Application

Metal injection molding is a shape forming process for producing complex, small parts in large quantities with low costs. MIM applications can already be found in such areas as medicine, computer, electronics and aerospace. A further wide field of applications is offered in automotive industry, where several possible MIM parts have been identified. [13] Examples of application for MIM components produced in Japan [12] are shown in Table 2.1.

Table 2.1 Types of steel for MIM components and their fields of application [12]

Classification	Type	Representative Application
Stainless	317L	Watch parts, medical parts
Austenite	316L	Waterworks parts
	17-4PH	Hard disk
Ferrite,	410L	Machine parts, machine tool parts
Martensite	440C	Thawing machines
Magnetic Fe-Ni	Kovar	Packages for sealing
Fe-Co	Permandure	Printer
Iron	2%Ni-Fe	Machine parts, leisure goods
	8%Ni-Fe	Machine parts
W	W-Cu	Heat sinks
Ti	Pure-Ti	Watch parts, accessories, leisure goods
High-speed steel	M2	Tools

Schlich et al [13] studied the development of valve needle for automotive fuel injection system by MIM. Processing details and advantages can be concluded as follow:

Powder 430L stainless steel with an amount up to 60 vol% and binder were kneaded in a sigma blade kneader to a compound. Then, the compound was injected. Thermal debinding was carried out in inert gas. The debound needles were sintered in Hydrogen at the temperature of 1260° C for holding time of 15 minutes. The density of 97% of theoretical density can be achieved.

MIM valve needles shows functional advantages against the conventionally manufactured needle as MIM needle effects better damping and less wear at the stop plate and at the valve seat. Latter guarantees a constant fuel flow through the valve which could enhance the life time of fuel injection valves.

Chapter 3

Experiment

3.1 Materials and apparatus preparation

3.1.1 Materials

3.1.1.1 Powder

Water atomised stainless steel powder grade 430L which produced by Pacific Metals CO.,LTD.   The average particle size is approximately 10 μm. Tap density is 4.35 g/cm^3. Chemical composition show in table 3.1.

Table 3.1 Chemical composition of stainless steel powder grade 430L

Symbol	Chemical Composition (%)								
	C	Si	Mn	P	S	Ni	Cr	Mo	Cu
Result	0.02	0.81	0.79	0.018	0.008	0.18	16.44	0.02	0.01

From : Mill Certificate by Pacific Metals Co.,LTD. Certificate No. F198D0112
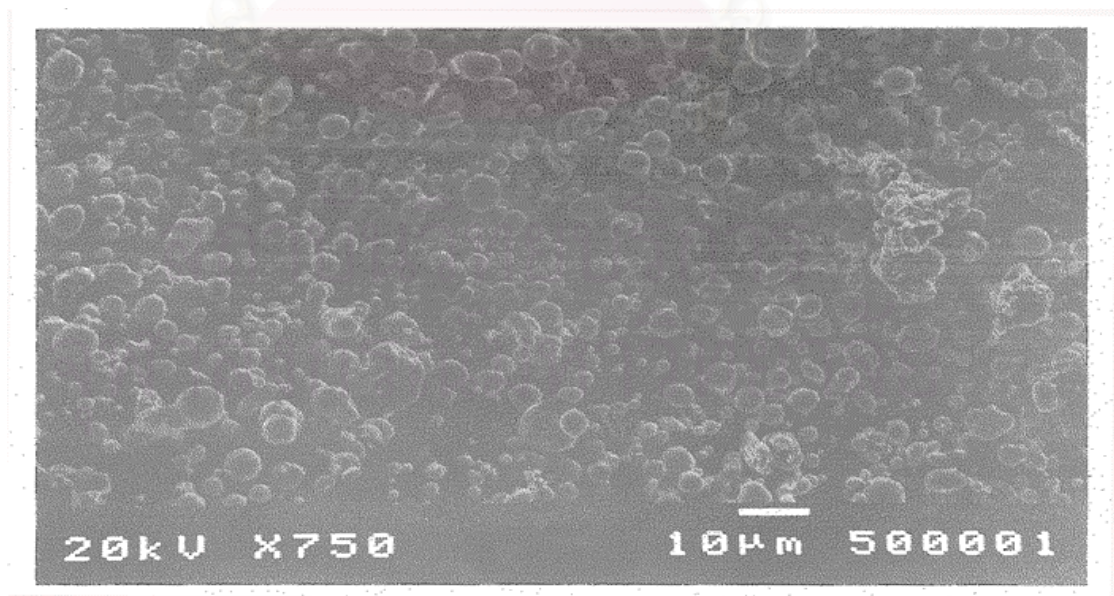
Figure 3.1 Scanning electron micrograph of water atomized 430L stainless steel powder

3.1.1.2   Binder

PAN-250 binder which produced by ADEKA Fine Chemical Co. compose of Natural wax, Fatty acid wax, Stearic acid, Poly-oxi-alkylen ether and Olefin-hydrocarbons. The binder has softening temperature of 85°C and density of 1.03 g/cm^3. TGA curve of PAN-250 is shown in figure 3.2. From TGA curve, PAN-250 decomposes in 2 ranges, 206.6-431.9°C (90.6%) and 431.9-500°C (7.4%).
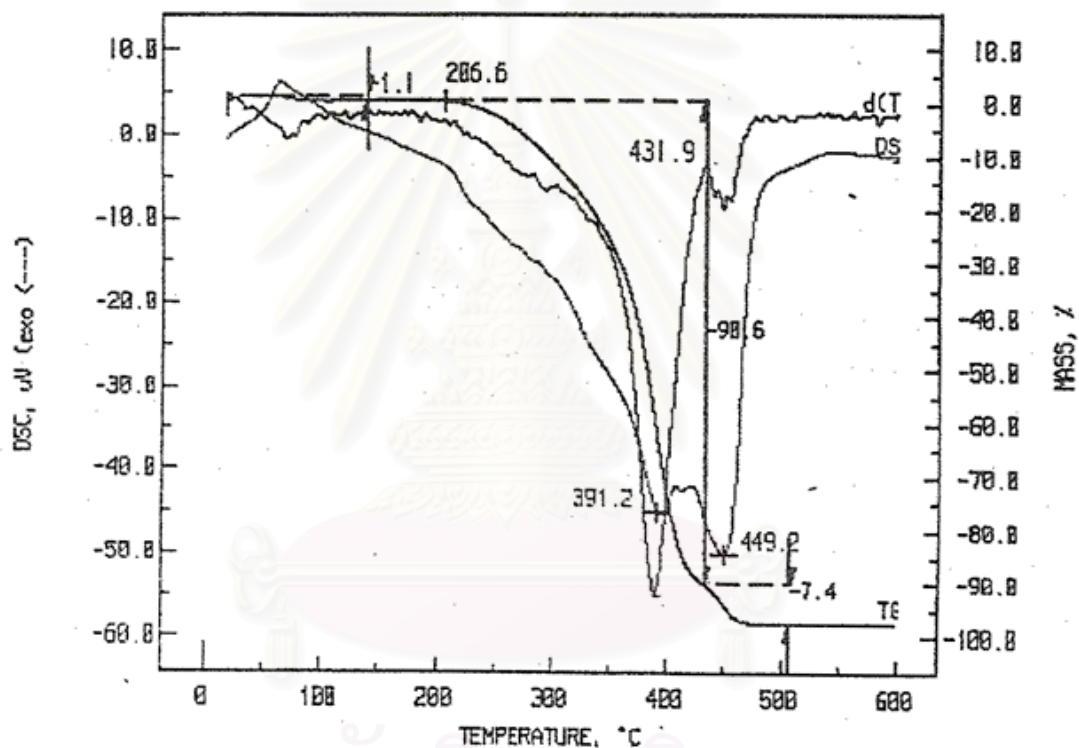
Figure 3.2 TGA curve of PAN-250

3.1.2   Apparatus preparation

Apparatus and equipment used in the experiment were shown in Table 3.2.

Table 3.2 Equipment used in the experiment

Equipment	Detail
1. Mixer	Designed and made in laboratory for using in premixing process
2. Kneader	KRC Kneader, Kuritomo Co.,LTD. Chemical Engineering Department
3. Die for tensile specimen	Gauge length 24mm and thickness 3mm
4. Die for Splined Coupling	Designed and made by Thai-German Institute
5. Injection molding machine	Model : BOY 15/5 No.4568
6. Debinding furnace	
6.1 Tube furnace	Stuart Scientific, Serial 004 Laboratory (LAB)
6.2 Tube furnace	Carbolite National Metal and Materials Technology Center (MTEC)
6.3 Muffle furnace	MEL, Japan
6.4 Furnace	ATOMIX COPERATION CO.,LTD. (ATOMIX)
7. Sintering furnace	
7.1 Batch furnace	Linn High Therm W. Germany King Mokut Institute Technology (KMIT)
7.2 Continuous furnace	Thai Sintered Products CO.,LTD. (TSP)
7.3 Vacuum furnace	Thai Tohken Thermo CO.,LTD. (TOHKEN)
7.4 Vacuum furnace	NEMS Model : NM-8 MEL, Japan
7.5 Vacuum furnace	ATOMIX COPERATION CO.,LTD. (ATOMIX)
8. Thermal Analyzer	
9. Vernia Caliper	
10. Rockwell Hardness Tester	SHIMADZU CORPORATION No. 29095648 Thai Tech Steel CO.,LTD.
11. Universal Tensile Tester	
12. Scanning Electron Microscope	
13. Microscope	Olympus

3.2 Experimental procedure

Conclusion experimental procedure was shown in figure 3.3.

```
┌──────────┐         ┌──────────┐
│  Powder  │         │  Binder  │
└────┬─────┘         └─────┬────┘
     └──────────┬──────────┘
           ( Premixing )
                │
            ( Mixing )
                │
          ┌──────────┐
          │ Compound │
          └────┬─────┘
        ( Injection Molding )
                │
          ┌──────────┐
          │ Compact  │
          └────┬─────┘
           ( Debinding )
                │
       ┌─────────────────┐
       │ Brown Specimen  │
       └────────┬────────┘
           ( Sintering )
                │
          ┌──────────┐
          │ Product  │
          └────┬─────┘
            ( Testing )
```
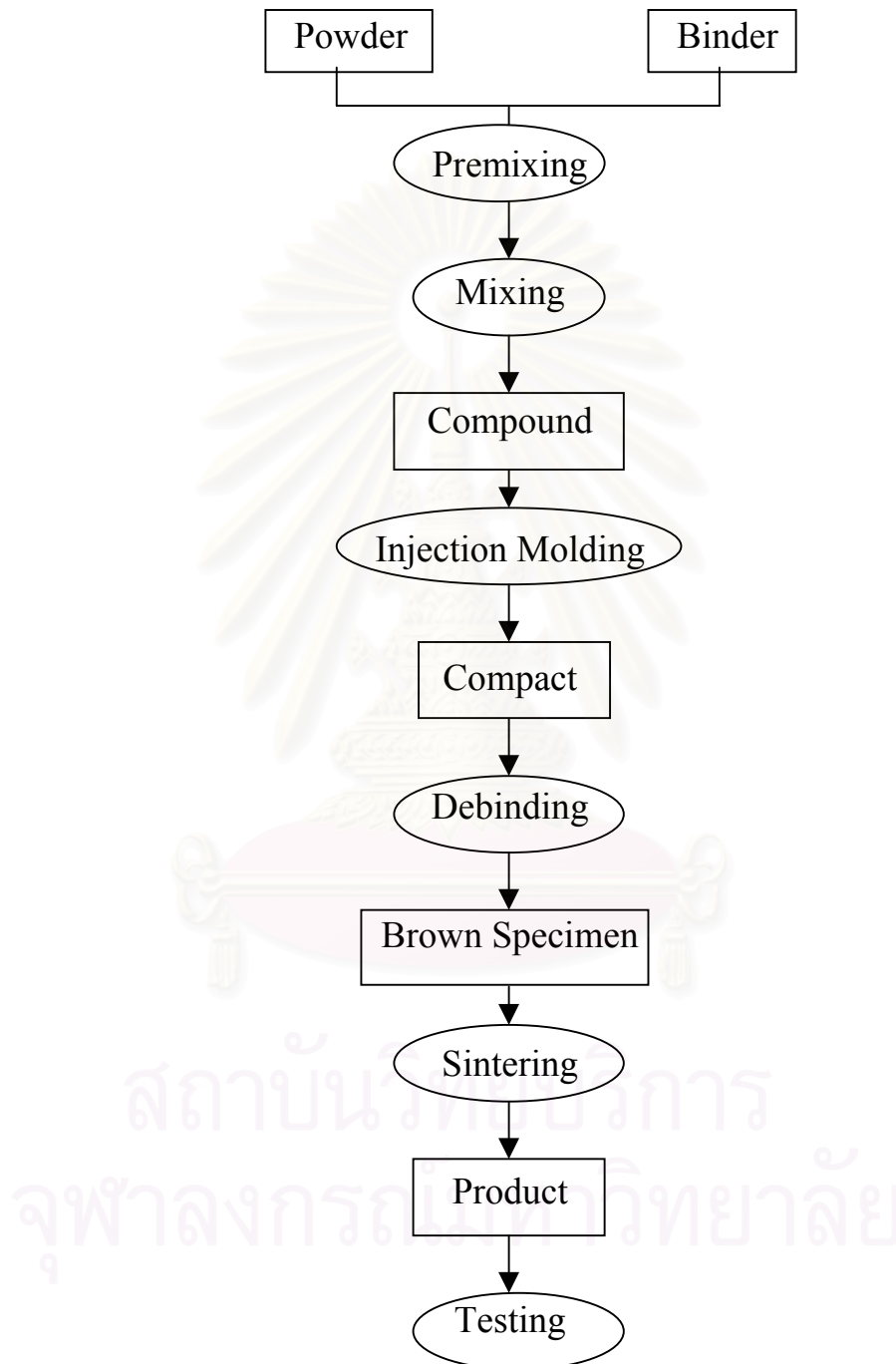
Figure 3.3 Flow chart of steps and experimental procedure

3.2.1 Fabrication

In the experiment, there are 2 formations of tensile specimens and splined couplings.

3.2.1.1 Mixing process

Powder with an amount up to 60 vol% and binder were mixed preliminary in a mixer. The premixing process has 4 steps :

1. put the binder PAN-250 into the mixer, then heat until it melt at the temperature of 120±5°C
2. turn the motor on at 100 rpm
3. put the powder progressively into the mixer
4. wait for 30 minutes, then put the premixed compound in aluminium foil

Since premixed compound was not homogeneous, it was subsequently mixed in kneader at the temperature of 120°C for 5 times in each batch with motor speed of 81, 122, 162 and 243 rpm. In each motor speed, ten samples were taken from different locations within the mixture. The densities of these samples were measured. The average density and standard deviation of each mixture were calculated. The optimized motor speed was selected.

3.2.1.2 Injection molding process

The mixed compound from optimized mixing condition was injected to be tensile specimens and splined coupling by plastic injection molding machine. Various conditions were tried. The successful condition was selected.

The successful condition for tensile specimen :
1. Injection pressure   = 70 bar
2. Injection temperature   = 110°C

The successful condition for splined coupling :
1. Injection pressure   = 100 bar
2. Injection temperature   = 130°C

After molding, the densities of three different positions of tensile specimens, i.e. gate area, middle area, and opposite of gate area and two different positions of splined couplings, i.e. gate area and opposite of gate area were measured. The pictures of tensile specimen and splined coupling were shown in figure 3.4 and 3.5 respectively.
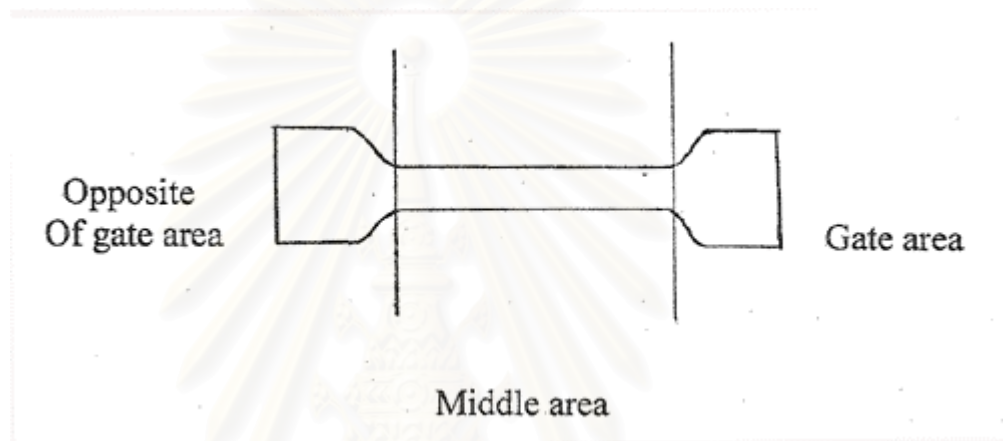
Figure 3.4 Tensile Specimen
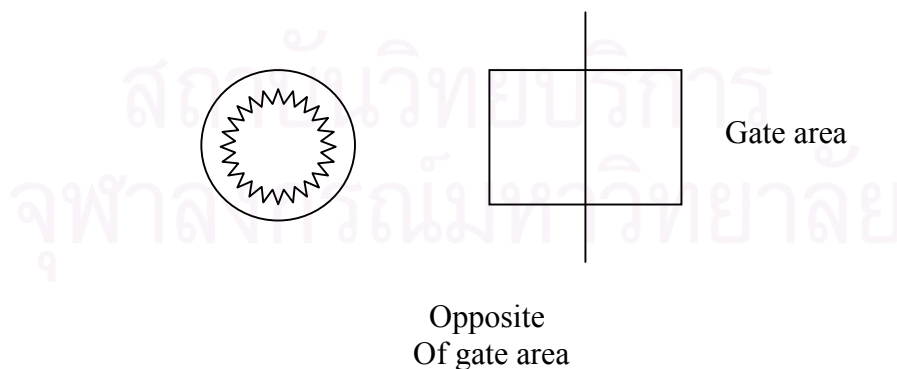
Figure 3.5 Splined Coupling

3.2.1.3   Debinding process

Tensile specimens and splined couplings were debound in various conditions. The conditions were shown in table 3.3.

Table 3.3 Debinding conditions

Debinding Condition	Heating Rate (°C/hr)	Temperature (°C)	Holding Time (Hr)	Atmosphere	Pieces	Place	For
1	12	280	18	Flow $O_2 <$ 1 l/min	6	MTEC	Tensile Specimen
2	12	280	40	Air	6	MTEC	Tensile Specimen
3	12	310	30	Flow Air< 1l/min	6	MTEC	Tensile Specimen
4	12	330	30	Flow Air < 1l/min	3	MTEC	Tensile Specimen
5	12	360	30	Flow Air < 1 l/min	9	MTEC	Tensile Specimen
6	12	400	24	Air	2	LAB	Tensile Specimen
7	12	450	31	Air	9	MTEC	Tensile Specimen
8	12	450	31	Fan	2	LAB	Tensile Specimen
9	12	450	20	Fan	3	LAB	Tensile Specimen

Table 3.3 Debinding conditions (continue)

Debinding Condition	Debinding schedule	Place	For
10	 Total Debinding time = 42 Hours Atmosphere = flow air with fan in muffle furnace	MEL, ATOMIX	Tensile Specimen And Splined Coupling
11	 Total Debinding time = 60 Hours Atmosphere = flow air with fan in muffle furnace	ATOMIX	Splined Coupling
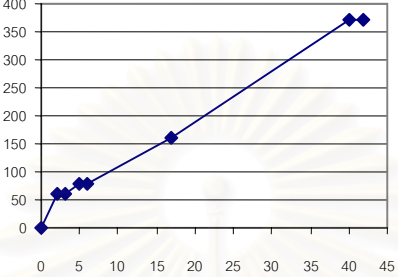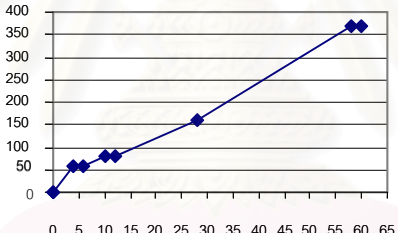
Specimens weight before and after debinding were measured. Then %extraction was calculated by equation:

$$\%extraction = \frac{(specimen\ weight\ before\ debind - specimen\ weight\ after\ debind) \times 100}{binder\ weight\ in\ the\ molded\ specimen}$$

3.2.1.4 Sintering process

Tensile specimens and splined couplings were sintered in various conditions. The conditions were shown in table 3.4.

Table 3.4 Sintering conditions

Sintering Condition	Debinding Condition	Temperature (°C)	Holding Time (min)	Atmosphere	Pieces	Place	For
1	2	1125	18	$N_2+70\%H_2$	3	TSP	Tensile Specimen
2	2	1195	180	$N_2+70\%H_2$	2	TSP	Tensile Specimen
3	4	1200	60	Vacuum (1 Tor)	3	TOHKEN	Tensile Specimen
4	2	1250	60	Ar	3	KMITT	Tensile Specimen
5	10	1250	60	H_2	2	MEL	Tensile Specimen
6	10	1300	60	H_2	3	MEL	Tensile Specimen
7	10	1350	60	H_2	3	MEL	Tensile Specimen
8	10,11	1290	180	Ar (1 Tor)	8	ATOMIX	Splined Coupling

3.2.2   Testing

3.2.2.1   Physical properties

Physical properties of sintered specimens were inspected.   The densities of tensile specimens and splined couplings were achieved by Archemedis Method.   Dimensions of tensile specimens shown in figure 3.6 were measured by vernia caliper to calculate %Shrinkage.   %Shrinkage was calculated by equation :

$$\%Shrinkage = \frac{\Delta l}{l\circ} \times 100\%$$
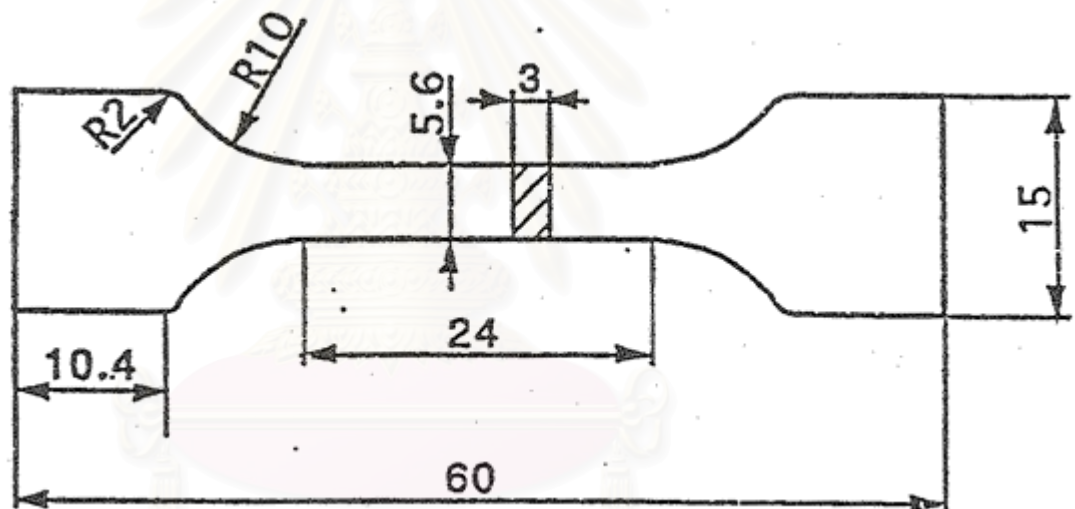
Figure 3.6 Dimension of tensile specimen

3.2.2.2   Mechanical properties

The hardness and tensile strength of the tensile specimens were inspected.   Rockwell scale B hardness tester was used with ball tip ϕ 1/16″ and load 100 kg.   Tensile tester was used at cross-head speed of 5 mm/s and load cell of 5 KN of maximum load.

3.2.3 Microstructure

To prepare surface of tensile specimens, sand paper number 400, 800, 1000, and 1200 were used. Then, the specimens were polished by 0.3 μm alumina and followed by alcoholic ferric chloride acid etching. The microscopic structure shows porosity and grain size.

Chapter 4

Result and Analysis

4.1 Mixing and injection molding

4.1.1 Results of mixing process

The average density and standard deviation of each motor speed were shown in table 4.1.

Table 4.1 Density of mixture

Condition (RPM)	Average Density (g/cm^3)	Standard Deviation	Homogeneity Ranking
81	4.534	0.179	4
122	4.697	0.065	1
162	4.571	0.085	3
243	4.524	0.084	2

The lowest deviation indicates the best homogeneity. [5] At motor speed of 122 rpm, the mixed compound had the lowest deviation and highest average density. Thus, the motor speed of 122 rpm was selected in the mixing process.

4.1.2   Results of injection molding process

The average density and standard deviation of different positions of the tensile specimens and splined couplings were shown in table 4.2. The photographs of injected tensile specimens and splined couplings were shown in figure 4.1 and 4.2 respectively.

Table 4.2 Density of tensile specimens and splined couplings

	Position	Average Density (g/cm^3)	Standard Deviation
Tensile Specimens	Opposite of gate area	5.051	0.034
	Middle area	5.048	0.031
	Gate area	5.035	0.064
Splined coupling	Opposite of gate area	4.982	0.032
	Gate area	4.984	1.201
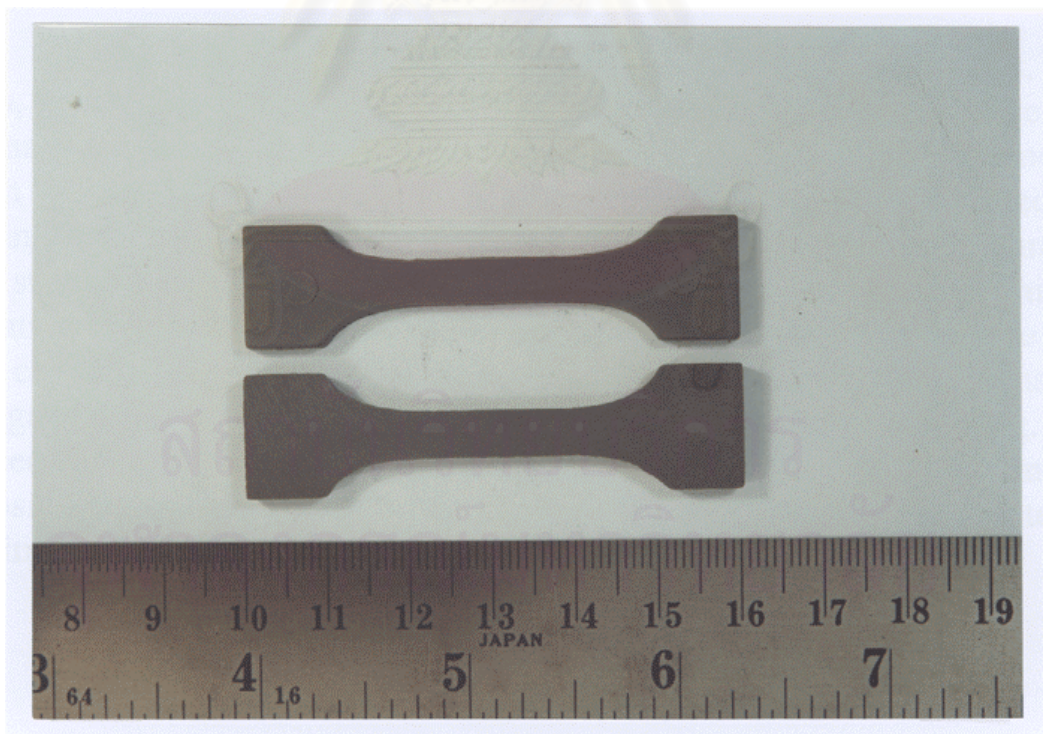
Figure 4.1 Photograph of injected tensile specimen
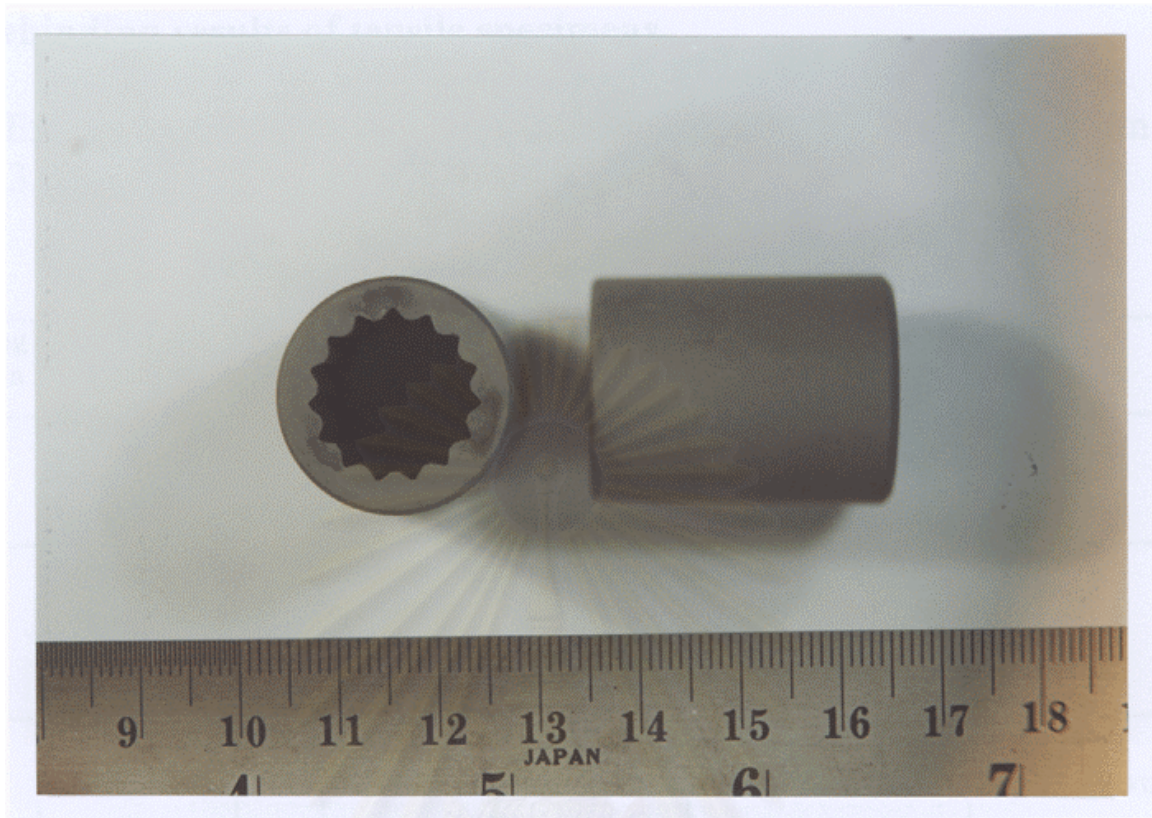
Figure 4.2 Photograph of injected splined coupling

In the other molding conditions, it can be found weld lines, short shots, cracks, sink marks, cavities and voids on the parts surface, and lamination cracks. At the successful molding condition, figure 4.1 and 4.2, it can be seen as a dark shade at gate area of both injected tensile specimen and injected splined coupling which indicates the binder-powder separation. The standard deviation at gate area of tensile specimens has the highest deviation which is about double of opposite of gate area and middle area. This can be assumed inhomogeneity of compact which result in dimensional changes that are not uniform and can lead to distortion in sintering. For splined coupling, the standard deviation at gate area is about 4 times of opposite of gate area. The inhomogeneity is more severe than the tensile specimens.

4.2 Debinding results of tensile specimens

%Extraction and appearance of debound specimens were shown in table 4.3.

Table 4.3 %Extraction and appearance of debound tensile specimens

Debinding Condition	Temperature (°C)	Time (Hr)	Atmosphere	%Extraction	Appearance	Color
1	280	18	Flow O₂ < 1 ml/min	> 98	Edge rounding, Slumping	Grey
2	280	40	Air	54-88	Stick to alumina substrate, blisters, surface cracks	Grey
3	310	30	Flow Air < 1l/min	96-98	Lamination cracks	Grey, Light brown
4	330	30	Flow Air < 1l/min	96-99	Lamination cracks	Light brown
5	360	30	Flow Air < 1l/min	94-96	Lamination cracks, surface cracks	Light brown, Grey
6	400	24	Air	100	Lamination cracks, blisters	Dark brown
7	450	31	Air	87-92	Lamination cracks, blisters, surface cracks	Dark brown, Black
8	450	31	Fan	100	Good	Grey, Light brown
9	450	20	Fan	> 98	Good	Grey, Light brown

Marks : All of the debound specimens has dimple at gate area.
There was an error of the change of %binder.

From the results, condition 8 and 9 were the successful conditions since the debound specimens have good appearance with grey and light brown color. At this condition, real temperature from thermocouple is about 330°C and atmosphere is flowing air with fan. However, the flow rate of air wasn't measured. This could be assumed that the specimens had good appearance at the optimum temperature and flow rate of atmosphere.

4.3 Sintering results of tensile specimens

Physical and mechanical properties of sintered specimens were shown in table 4.4 and 4.5 respectively.

Table 4.4 Physical properties of sintered tensile specimens

Sintering Condition	Temperature (°C)	Average %Shrinkage	Average Density	
			g/cm³	%
1	1125	6.89	-	-
2	1195	11.19±0.93	6.710±0.180	86.03±2.36
3	1200	12.39	6.87	88.08
4	1250	-	-	-
5	1250	13.53±0.43	7.428±0.021	95.23±0.26
6	1300	14.04±0.28	7.474±0.011	95.82±0.14
7	1350	14.23±0.21	7.469±0.020	95.75±0.26

From the results, condition 1 and 4 were not successful since the specimens had shrinkage of only 6.89% in condition 1 and had no shrinkage in condition 4 . Condition 3 was not constant since the specimens were not sintered in the latter experiments. The specimens from condition 2, 5, 6, and 7 were selected to test mechanical properties.

Table 4.5 Mechanical properties of sintered tensile specimens

Sintering Condition	Temperature (°C)	Average HRB	Stress (MPa)		%Strain at Auto Break
			Ultimate	Offset Yield	
2	1195	95.60±0.00	339.39±39.24	61.11±7.86	6.34±0.41
5	1250	72.71±0.19	395.49±2.12	256.25±16.24	21.33±2.03
6	1300	73.19±0.66	395.03±5.56	225.78±13.35	24.59± 2.18
7	1350	70.35±3.89	399.37±6.28	244.22±25.38	22.54±2.88

Since sintered specimens in condition 5, 6, and 7 had similar pore structure and microstructure, the sample of the structures were shown in figure 4.3 and 4.4. The pore structure and microstructure of sintered specimens in condition 2 were shown in figure 4.5 and 4.6. Average grain size, maximum porosity size and porosity shape were shown in table 4.6.

Table 4.6 Porosity and grain size of sintered tensile specimens

Sintering Condition	Temperature (°C)	Average Grain size (μm)	Maximum Porosity size (μm)	Porosity shape
2	1195	-	-	Irregular
5	1250	55.56	22.5	Round
6	1300	62.50	17.5	Round
7	1350	62.50	12.5	Round

Figure 4.3 Pore structure of a tensile specimen which sintered at 1350°C
in hydrogen atmosphere (x200)
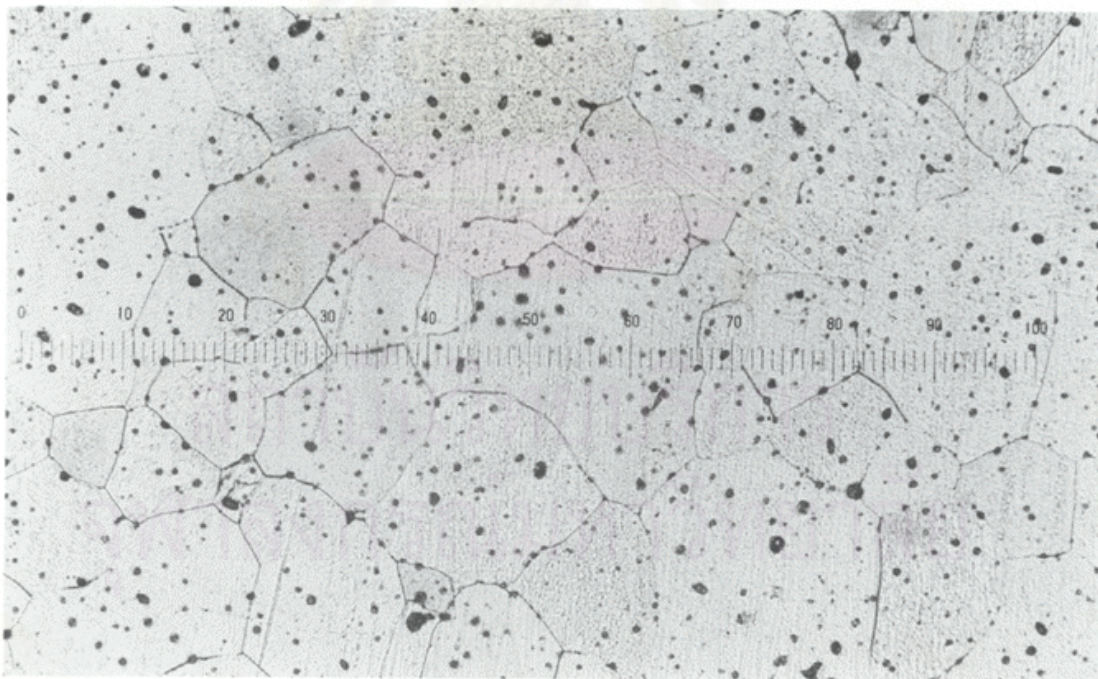
Figure 4.4 Microstructure of a tensile specimen which sintered at 1350°C
in hydrogen atmosphere (x200)

Figure 4.5 Pore structure of a tensile specimen which sintered at 1195°C
in N_2+70%H_2 atmosphere (x200)

Figure 4.6 Microstructure of a tensile specimen which sintered at 1195°C
in N_2+70%H_2 atmosphere (x200)

4.4 Sintering results of splined couplings

The average density of sintered splined couplings was shown in table 4.7. The photographs of splined couplings were shown in figure 4.7 and 4.8.

Table 4.7 Density of splined couplings

Debinding Condition	Sintering Condition	Density	
		g/cm^3	%
10	8	6.618±0.064	84.85±0.82
11	8	6.543±0.125	83.88±1.60

Figure 4.7 Photograph of splined coupling which debound in condition 10
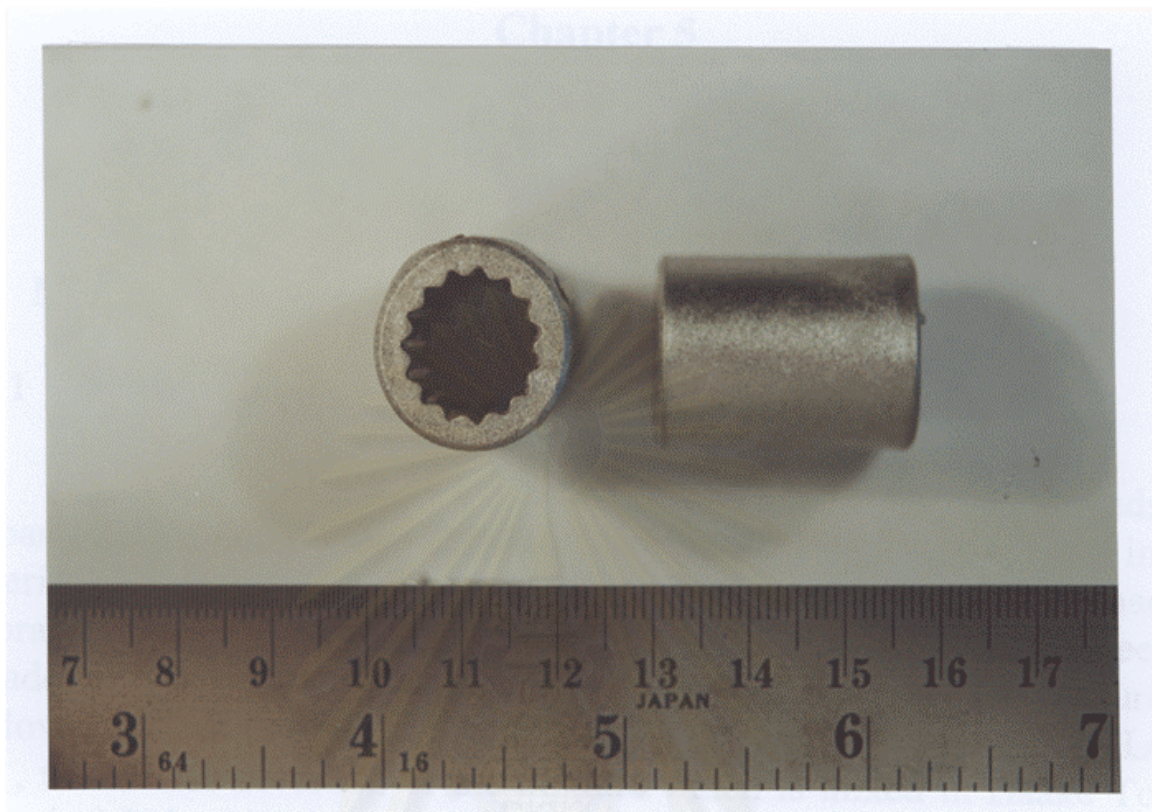
Figure 4.8 Photograph of splined coupling which debound in condition 11

Chapter 5

Discussion

5.1 Mixing and injection molding

5.1.1 Effect of mixer in mixing process

Normally, several high-shear mixers are used for MIM feedstock preparation. There is no high-shear mixer in laboratory, thus, in the experiment, powder and binder were mixed in a mixer which was made in laboratory and subsequently mixed in a kneader. The motor speed of kneader of 122 rpm was selected in the mixing process since the mixture has the lowest deviation of 0.065. However, to compare with the study of Loh et al [5], the lowest deviation of the mixture which is mixed in Haake Torque mixer is 0.010 which is much lower.

From the experiment, the feedstock could be premixed in a mixer and subsequently mixed in a kneader.

5.1.2 Surface defects of injection molded parts

Before the successful conditions of tensile specimens and splined couplings were selected, the other molding conditions were tried. In the other molding conditions, several defects were found, i.e. weld lines, short shots, cracks, sink marks, cavities and voids on the parts surface, and lamination cracks. These defects could be eliminated through adjustments of the time, temperature, and pressure of the molding process.

Short shots, sink marks, and cavities and voids on the compact surface were caused by solidification of the feedstock before it fills the cavity and insufficient mass in the mold to offset shrinkage contraction during cooling. Usually, they can be cured by decreasing temperature, increasing injection speed, or modifying pressure profiles. In the experiment, these defects were eliminated by using lower temperature.

The shear stress which varies across the flow path can lead to separation of the powder and binder at the die wall. Because of these flow lines and packing gradients, the compacts can exhibit laminated cracks. In this experiment, laminated cracks were eliminated by using higher molding temperature and faster filling time.

Weld lines could be found in injection molding of splined couplings more often than tensile specimens. It appeared when free surfaces of the injected fluid meet the mold surface at reduced temperature. It can also be formed if the feedstock flows around an obstacle like a core rod. [6] Usually, this problem can be eliminated by modifying the cavity design of the mold, decreasing the viscosity of the feedstock, or preventing the cooling of the flow front by increasing the temperature of the feedstock and the mold. In the experiment, weld lines were eliminated by increasing the molding temperature to 130°C for splined couplings.

The binder-powder separation can not be eliminated in the experiment. It occurs when the cross-section of the molded geometry changes significantly. [6] From figure 4.1 and 4.2, it can be seen as a dark shade at gate area which indicates binder-powder separation. The separation causes non-uniform density as there is a large density difference between powder and binder. From table 4.2, the density at gate area is lower than others and deviation is about double of the other areas. This causes a dimple at the gate area during debinding. Increasing the gate size and decreasing the injection speed to a proper level can minimized the separation. [6] In the experiment, the injection speed were decreased which caused the decreasing of dark shade area.

Average density and standard deviation at different positions of splined coupling shown in table 4.2 indicated inhomogeneity of compact resulting in distortion of sintered specimens shown in figure 4.7 and 4.8. The deviation at gate area was about 4 times of the opposite of gate area which the inhomogeneity was more severe than the tensile specimens. This is because splined couplings had more complex shape than tensile specimens.

5.2 Debinding of tensile specimens

5.2.1   The problems of specimens before debinding

5.2.1.1   %Extraction

From debinding results, most debound specimens had %extraction of 94-99% but, some debound specimens had %extraction of 100%. This may be explained in 2 reasons.

First, the binder used in the experiments was 40 vol% or 8.8 wt%. It is possible that some powders were lost in a mixer and equipment in mixing process which caused increasing of the binder to more than 8.8 wt%.

Second, in debinding process, %extraction was calculated by equation :

%extraction   = (specimen weight before debind – specimen weight after debind) x 100
                        binder weight in the molded specimen

Some powders may lose during debinding. Since, %extraction were calculated by specimen weight before debind – specimen weight after debind, the lost powder weight were included in the lost binder weight.

5.2.1.2   Binder-powder separation

Some debinding defects were found in the experiment such as dimple at gate area. This defect could be traced to molding process. The binder-powder separation in molding process caused dimple at gate area during debinding.

5.2.1.3   Cracks

Surface cracks in debinding process were found around the ejection area. The ejection area was shown in figure 4.1. At this area, the tensile specimens received external forces from ejection pin to release the specimens from the mold. This caused surface cracks.

5.2.2   Effect of debinding temperature on %extraction and appearance

From TGA curve, PAN-250 decomposes in 2 ranges, 206.6°C-431.9°C (90.6%) and 431.9°C-500°C (7.4%).   Several temperatures were selected to use in the experiment. A very slow heating rate of 12°C/hr was used to heat the specimens to the debinding temperature.   However, there was no step of debinding temperature.

Temperature of 400°C and 450°C were too high to debinding because the specimens were burnt and had dark brown color.   While, the temperature of 280°C was not enough to debinding since %extraction was only 54-88% and the specimens stuck to alumina substrate due to remained binder.   The temperature of 360°C, 330°C and 310°C, the specimens had good %extraction of 94-99%.   The temperature of 310-360°C was the successful debinding temperature.

The remained binder is to hold the particle together for handle the specimens and can be eliminated in sintering process.

5.2.3   Effect of debinding atmosphere on %extraction and appearance

In the experiment, three oxidizing atmospheres, i.e. oxygen, air with flow rate less than 1 l/min, and flowing air with fan were used.   Oxidizing atmosphere aid in breaking apart the wax molecules and remove residual carbon.   However, it will alter the surface chemistry of the powder and exothermic reactions between the binder and oxygen can lead to temperature control problems.

The specimens which debound in oxygen have edge rounding and slumping.   The oxygen had too much reaction with the binder at surface of the specimens which caused the fall of powder from surface of the specimens.   Thus, oxygen was not good for debinding.

The specimens which debound in air with flow rate less than 1l/min had lamination cracks.   While, the specimens which debound in flowing air by fan had good appearance. Flowing air by fan had flow rate more than air with flow rate less than 1l/min.   However, the flow rate of fan was not measured. Flowing gas is used to transport vapors from the furnace.   Higher

flow of debinding gas enhances the evaporation of low molecular weight components.

5.3 Sintering of tensile specimens

5.3.1 Microstructure

Figure 4.3 and 4.4 showed the pore structure and microstructure of the tensile specimens which sintered at 1350°C in Hydrogen. It could be found that the part had small pore size and round shape of pores. From table 4.6, the specimens which sintered in higher temperature had larger grain size due to the coarsening of the microstructure. The grain growth occurred. Maximum porosity size of the specimens which sintered at 1350°C was smallest which means in the final stage of sintering, the sintering was more complete at higher temperature.

Figure 4.5 and 4.6 showed the pore structure and microstructure of the tensile specimens which sintered at 1195°C in $N_2+70\%H_2$. It could be found that the pores had irregular shape which mean the sintering was not complete.

5.3.2 Effect of sintering temperature on physical and mechanical properties

From the results, the tensile specimens which sintered in Japan at the temperature of 1250°C, 1300°C, and 1350°C had nearly the same physical properties, i.e. shrinkage and density, and mechanical properties, i.e. hardness, tensile strength, and %elongation. This was because they had nearly the same amount of porosity and the same shape of round pores.

At the temperature of 1250°C, the sintering reached the final stage. At the final stage of sintering, the isolated pores occurred. The elimination of isolated pores is difficult, since vacancies must diffuse for long distance to the surface, which is very slow process. This caused the amount of porosity of the specimens sintered at 1250°C, 1300°C and 1350°C were almost the same.

In this study, sintering of 430L stainless steel powder at the temperature of 1350°C for 60 minutes in hydrogen atmosphere can achieved the density of 7.469 g/cm^3 which is 95.75% of theoretical density and ultimate tensile strength of 399.37 MPa. Comparing to the study of Loh et al [10], sintering of 316L stainless steel powder at the temperature of 1350°C for 60 minutes in vacuum atmosphere can achieved the density of 7.449 g/cm^3 which is 94.29% of theoretical density and ultimate tensile strength of 338.9 MPa.

The specimens which sintered at 1195°C in N_2+70%H_2 atmosphere had much lower shrinkage, density, tensile strength and %elongation but higher hardness than those sintered at 1250°C, 1300°C and 1350°C in hydrogen atmosphere. From microstructure, they had irregular shape of pores which means the sintering was not as complete as the specimens sintered at 1250°C, 1300°C and 1350°C. The pores was irregular shape and the density was only 86.03% of theory density due to the sintering was not reached final stage at the temperature of 1195°C.

However, the specimens sintered at 1195°C had higher hardness of 95.60 HRB. The higher hardness may due to chromium nitride which could be formed via the reaction, $2Cr + 1/2N_2 \rightarrow Cr_2N$, since the chromium which is 16.44% content in the 430L stainless steel powder may react with the sintering atmosphere of N_2+70%H_2. The atmosphere of N_2+70%H_2 came from dissociated ammonia and 5% of nitrogen. The ammonia molecule was broken into hydrogen and nitrogen. The hydrogen provided for oxide reduction and the nitrogen reacted to form nitride. From the XRD results showed in appendix B, the tensile specimen sintered in hydrogen atmosphere did not have chromium nitride, while the tensile specimen sintered in N_2+70%H_2 had chromium nitride. The chromium nitride may also cause the unusually high of ultimate tensile strength of 339.39 MPa and unusually low %elongation of 6.34%. From the stress-strain curve of the specimen sintered in N_2+70%H_2 showed in appendix A, the ultimate point and the fracture point were the same point which characterized the brittle behavior of the materials.

5.4   Debinding and sintering of splined couplings

From table 4.8, splined couplings which debound in condition 10 and 11 had nearly the same density since they were sintered in the same condition at 1290°C.

Splined couplings which debound in condition 10 had more remained binder than those debound in condition 11 since the total time of debinding condition 10 is 42 hours which is much shorter than total time of debinding condition 11 which is 60 hours. Debinding condition 10, time may not enough to remove most of the binder. A lot of remained binder was trapped within the splined coupling and was removed in the sintering process which result in distortion in sintering. Thus, the sintered splined couplings which debound in condition 10 is more distortion than those debound in condition 11. The sintered splined couplings were shown in figure 4.7 and 4.8.

Since the sintered splined couplings had some distortions due to much dimensional changes, they could not use in actual work. This dimensional control problem can be decreased by using some methods such as :
1. Using post-sintering process of sizing
2. Using infiltration such as copper and bronze [14]

Chapter 6

Conclusion and suggestion

6.1 Conclusion

1. Powder 430L stainless steel and binder PAN-250 can be mixed in kneader at the temperature of 120°C with motor speed of 122 rpm.

2. The successful molding condition for tensile specimens is injection pressure of 70 bar and injection temperature of 110°C and the successful molding condition for splined couplings is injection pressure of 100 bar and injection temperature of 130°C. At these conditions, the specimens had no other defects except binder-powder separation at gate area.

3. The successful debinding condition for tensile specimens is the debinding temperature of 310-360°C in flowing air with fan for holding time of 30 hours which achieved %extraction of 94-99%.

4. Sintering temperature of 1250°C, 1300°C and 1350°C in hydrogen atmosphere, the specimens had nearly the same physical properties, i.e. shrinkage and density, and mechanical properties, i.e. hardness, tensile strength, and %elongation. The maximum density of 95.82% of theoretical density and ultimate tensile strength of 399.37 MPa can be achieved. Sintering temperature of 1195°C in N_2+70%H_2, the sintering was not complete and the specimens had density of 86.03% of theoretical density.

5. Comparing to the specimens sintered in hydrogen atmosphere, the specimens sintered in N_2+70%H_2 had higher hardness of 95.60 HRB, and lower %elongation of 6.34%. The specimens behaved brittle due to Cr_2N from the reaction of chromium in stainless steel powder and sintering atmosphere of dissociated ammonia.

6. The splined couplings can be formed though MIM process. However, sintered splined couplings had some distortions resulting in dimensional control problem.

6.2 Suggestion

1. Study debinding parameter, i.e. debinding atmosphere, and flow rate of debinding atmosphere in thermal debinding process.

2. Study other debinding methods such as solvent debinding to decrease debinding time.

3. Further study of splined coupling to decrease dimensional control problem such as study infiltration such as copper and bronze, debinding time, and post-sintering process.

References

1. German, R. M.; and Cornwall, R. G. Worldwide Market and Technology for Powder Injection Molding. <u>The International Journal of Powder Metallurgy</u> 33 (Jun-Jul 1997) : 23-27.
2. White, D. G. Powder Metallurgy in North America. <u>Materials Technology</u> 11 (Nov-Dec 1996) : 242-245.
3. Whittaker, D. Process Economics and Technological Advances in P/M Automotive Parts. <u>The international Journal of Powder Metallurgy</u> 34 (1998) : 53-62.
4. German, R. M. Powder Injection Molding. Metal Powder Industries Federation: 1990.
5. Loh, N. H.; Tor, S. B.; and Khor, K. A. Powder Injection Molding – Mixing Study Using Taguchi Method. <u>3rd International Symposium on High Performance Metal Matrix Composites</u> (March 1999) : 216-227.
6. Ji, C. H.; Loh, N. H.; Tor, S. B.; and Khor, K. A. Investigation of Metal Injection Molding (MIM) Defects. <u>3rd International Symposium on High Performance Metal Matrix Composites</u> (March 1999) : 228-239.
7. Hwang, K. S.; and Tsou, T. H. Thermal Debinding of Powder Injection Molded Parts - Observations and Mechanisms, <u>Metallurgical Transactions A</u> 23A (1992) : 2775-2782.
8. Moore, J. A.; Jarding, B. P. ; Lograsso, B. K.; and Anderson, I. E. Atmosphere Control during Debing of Powder Injection Molded Parts. <u>Journal of Materials Engineering and Performance</u> 4 (1995) : 275-282.
9. Ji, C. H.; Loh, N. H.; Khor, K. A.; and Tor, S. B. Effects of Debinding Parameters on Metal Injection Molding Parts. <u>3rd International Symposium on High Performance Metal Matrix Composites</u> (March 1999) : 205-215.
10. Loh, N. H.; Khor, K. A.; and Tor, S. B. Metal Injection molding of stainless steel 316L. <u>2nd International Symposium on High Performance Metal Matrix Composites</u> (1997) : 262-272.
11. Ji, C. H.; Loh, N. H.; Khor, K. A.; and Tor, S. B. Sintering Study of 316L Stainless Steel MIM Parts Using Taguchi Method:Final Density. <u>3rd International Symposium on High Performance Metal Matrix Composites</u> (March 1999) : 240-264.

12 Yoshiyuki, K. Ultrafine Powder of Metal Injection Molding (MIM) of Automobile Parts. Pacific Metal (n.p.,n.d.) : 1-9.

13 Schlich, H. F.; and Schelb, B. Development of Valve Needle for Automotive Fuel Injection System by MIM. Powder Injection Molding Symposium (1992) : 481-492.

14 Velasco, F.; Torralba, J. M.; Ruiz-Roman, J. M. et al. Effect of Infiltration on The Mechanical Properties and Corrosion Resistance of Austenitic Stainless Steels. The international Journal of Powder Metallurgy 31 (1995) : 309-315.
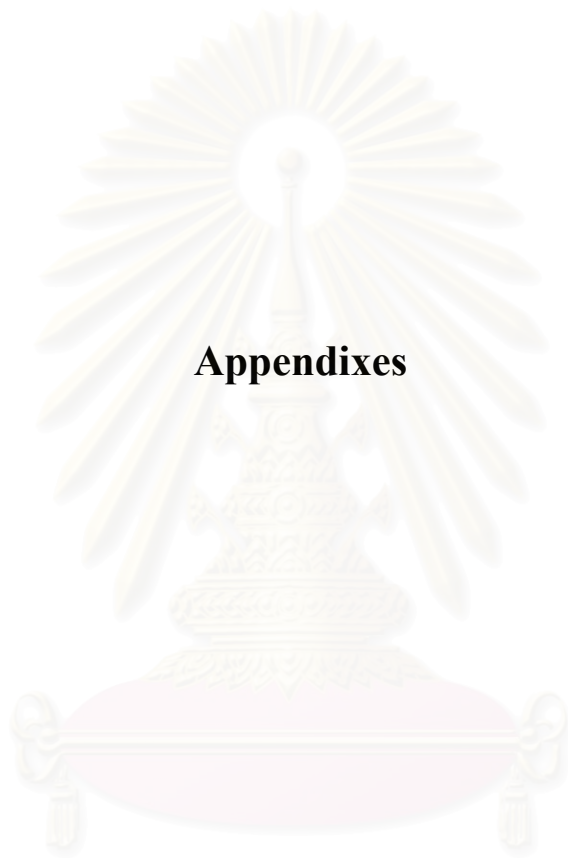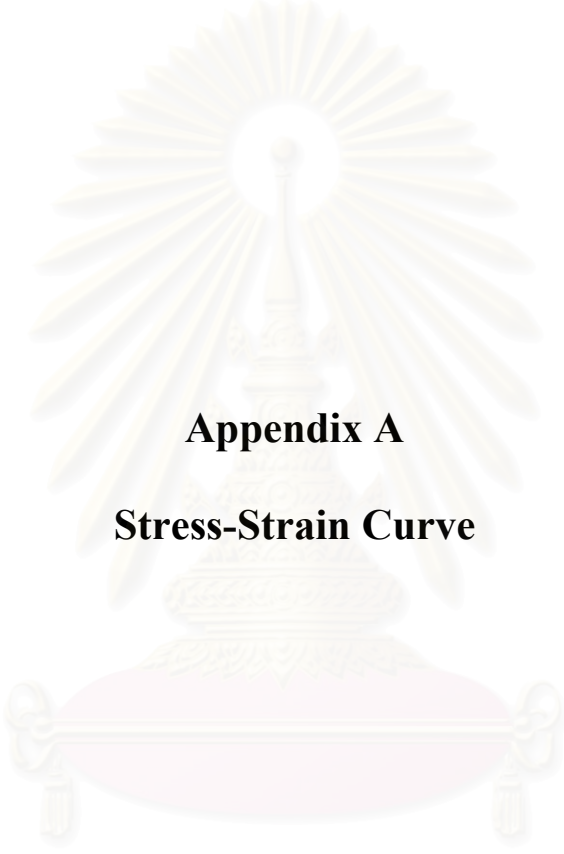
Appendixes

Appendix A

Stress-Strain Curve

Stress-strain curve of tensile specimen sintered at 1300°C in hydrogen atmosphere
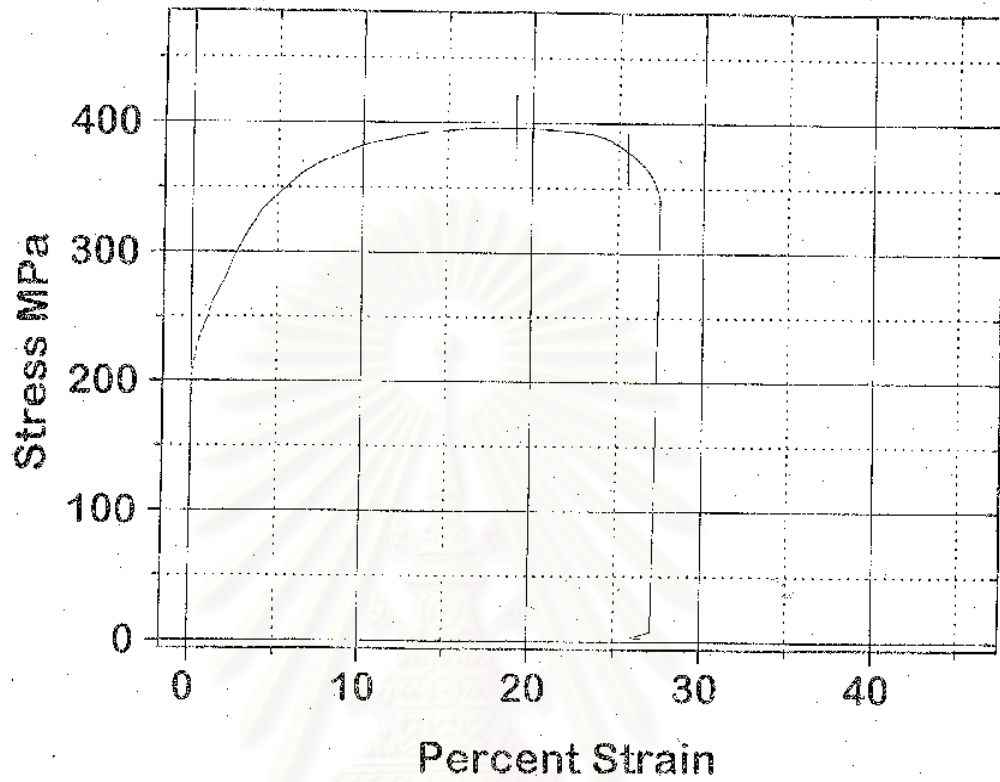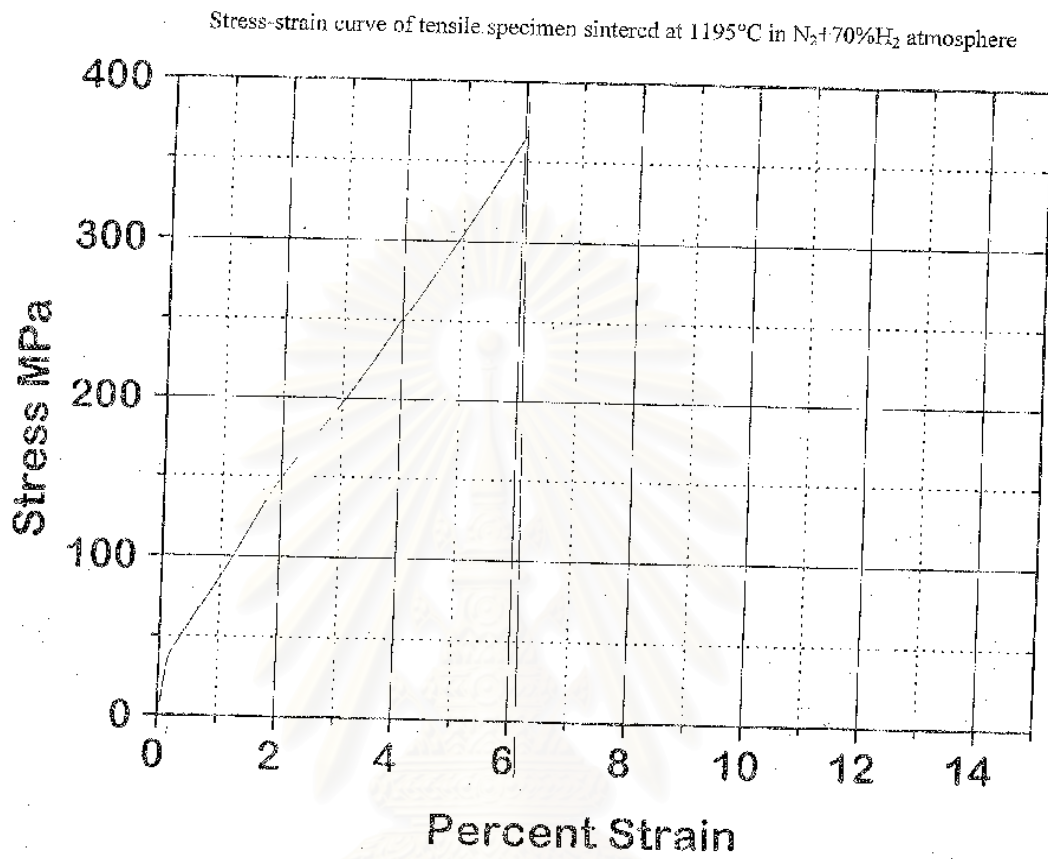
Stress-strain curve of tensile specimen sintered at 1195°C in N_2+70%H_2 atmosphere

Appendix B

XRD Results
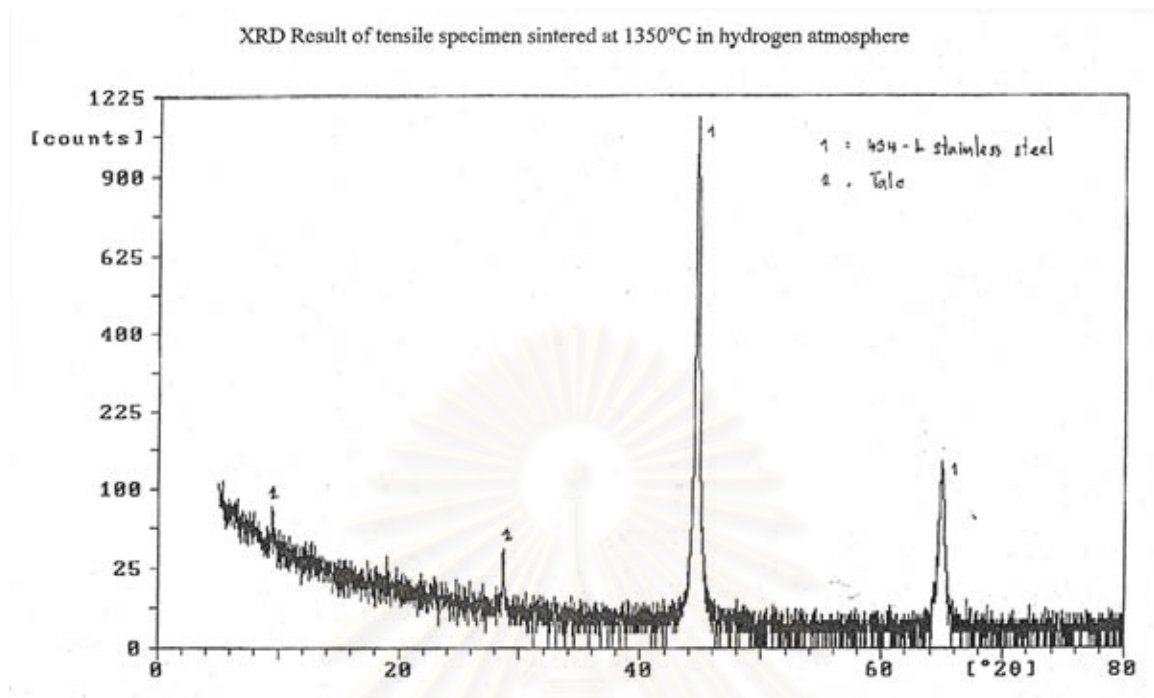
XRD Result of tensile specimen sintered at 1350°C in hydrogen atmosphere

XRD Result of tensile specimen sintered at 1195°C in N_2+70%H_2 atmosphere

1 = Chromium Nitride
2 = Alabandite
3 = 434-L stainless steal
4 = Copper
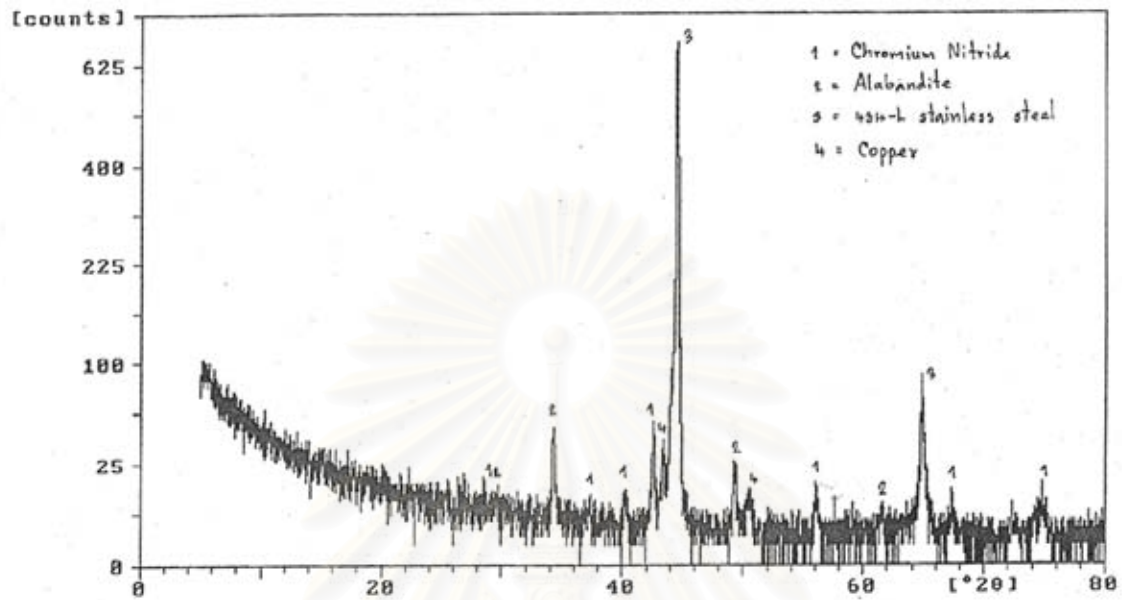
Biography

Miss Adikarn Tongsa-ad was born on November 1, 1976 in Bangkok, Thailand. She received a B.Eng. from Metallurgical Engineering Department, Engineering Faculty, Chulalongkorn University in 1997. She began to study master degree in Metallurgical Engineering at Chulalongkorn University in 1997.